J Solid State Electrochem (2006) 10: 995–1001
DOI 10.1007/s10008-005-0045-3

ORIGINAL PAPER

Guo-Qing Zhang · Xiao-Gang Zhang · Hu-Lin Li

Self-assembly preparation of mesoporous hollow nanospheric manganese dioxide and its application in zinc-air battery

Received: 26 April 2005 / Revised: 1 June 2005 / Accepted: 24 June 2005 / Published online: 20 September 2005

Abstract In this work, mesoporous manganese dioxide with novel hollow nanospheric structure was prepared by a facile, template-free self-assembly process at room temperature in a short period of time. The product was characterized by X-ray diffraction, scanning electron microscopy, and energy-dispersive X-ray spectroscopy. The results indicate that the as-prepared material has a special mesoporous hollow nanospheric morphology and a typical composition of γ-MnO_2. Polarization curve, chronoamperometry and Tafel plot tests demonstrate that this nanostructured material has high electrocatalytic activity for the reduction of dioxygen compared to commercial electrolytic MnO_2 (EMD). Electrochemical impedance spectroscopy that was analyzed by equivalent circuit shows that as-prepared MnO_2-catalysted air electrode has a small contact resistance and ohmic resistance, a low value of electrochemical polarization resistance. An all solid-state zinc-air cell has been fabricated with this material as electrocatalyst for oxygen electrode and potassium salt of cross-linked poly(acrylic acid) as an alkaline polymer gel electrolyte. The cell has a better discharge characteristic than that of the cell employing EMD at room temperature.

Keywords γ-MnO_2 hollow nanosphere · Air-electrode electrocatalyst · Zinc-air cell · Equivalent circuit

G.-Q. Zhang · H.-L. Li (✉)
Chemistry Department, Lanzhou University, Lanzhou, 730000 China
E-mail: zhangguoq04@st.lzu.edu.cn
Tel.: +86-931-8912517
Fax: +86-931-8912582

X.-G. Zhang
College of Material Science & Engineering, Nanjing University of Aeronautics and Astronautics, Nanjing, 210016 China

Introduction

The high-performance electrocatalysts for air cathode is playing an important role in the development of metal-air battery or fuel cells. During the past decades, various inexpensive electrocatalysts such as metal phthalocyanines and porphyrins [1–3], perovskite metal oxides [4–5], and manganese oxides [6–11] were explored as a replacement for platinum. Among the low-cost electrocatalysts investigated, manganese oxide seems to be the most promising candidate due to its lower cost and higher catalytic performance for oxygen electroreduction.

The catalytic activity of manganese oxide is closely related to the electrochemical activities of MnO_2 [12]. Among various types of manganese oxides, an electrochemically active form is γ-MnO_2; this form of manganese oxide has been commercially used as cathode materials in alkaline batteries. So, γ-MnO_2 is the most favorable form of manganese oxide for oxygen electroreduction.

The structure of γ-MnO_2 is considered to be a random intergrowth of 1×1 tunnels of pyrolusite and 1×2 tunnels of ramsdellite, which are constructed of MnO_6 octahedral units with edge or corner sharing [13–14]. γ-MnO_2 can be conventionally prepared by electrochemical oxidation of acidic $MnSO_4$ solution as well as by chemical methods, however, these powdered particles prepared in usual methods have irregular morphologies [15] and the surface area is less than 80 m^2/g [16].

Redox precipitation process involving oxidation of Mn^{II} salts and/or reduction of MnO_4^- salts in solution is a typical method for the preparation of synthetic manganese oxides, as we know, using permanganate as oxidation agent, the as-obtained product always contain various kind of metal cations. Because different morphologies and surface area are generally believed to be responsible for MnO_2's electrochemical performance [17], here, we chose silver permanganate as the manganate salt, prior to use this manganate salt to react with

Mn^{Π} salt, using reaction between hydrochloric acid and silver permanganate, Ag^{+} ions in permanganate was separated as AgCl and fresh permanganic acid was obtained, then diluted $MnSO_4$ was reacted with permanganic acid at room temperature to prepare pure γ-MnO_2, which has a special morphology and high surface area. Air electrodes containing as-prepared γ-MnO_2/or commercial electrolysis MnO_2 (EMD) as electrocatalysts were fabricated successfully, and their electrocatalytic performances were compared by electrochemical measurements in alkaline environment.

Experimental

In this process, we use diluted $MnSO_4{\cdot}H_2O$ reacted with permanganic acid at room temperature to prepare γ-MnO_2. Fresh permanganic acid must be prepared prior to use and is made by reacting hydrochloric acid with silver permanganate. To prevent undesirable byproducts, silver permanganate was chosen as the manganate salt. Silver permanganate was purchased from Aldrich with no other treatment before use. Silver chloride is insoluble in water, thus preventing metallic ions from entering synthetic structure. The preparation was as follows.

First 5 mL of 0.5 M HCL was added dropwise to 100 mL of 0.025 M $AgMnO_4$ solutions. After being vigorously stirred at room temperature for 10 min, the solution was centrifuged and decanted. The resultant pink solution was added dropwise into 300 mL of 0.02 M $MnSO_4{\cdot}H_2O$ solutions while being rapidly stirred for 12 h at room temperature. The obtained slurry was filtered and washed with distilled water at least four times and then dried in air at 120 °C for an additional 12 h. The final product was black powder.

Structure characterization of the as-prepared manganese oxide was performed by means of X-ray diffractometer (MAC M18XCE) with Cu K_α radiation ($\lambda = 1.54056$ Å) operating at 50.0 KV and 200.0 mA, employing well-ground samples at a scan rate of 10 °/min in order to obtain precise diffraction patterns with appropriate intensities. Morphology of the manganese oxide was investigated by scanning electron microscopy (SEM) (Leo1430VP) investigations. TEM specimens were prepared by dispersing the powder in alcohol by ultrasonic treatment, dropping onto a copper gridding mesh, and then dried in air. Element analysis of the resulted powder was performed by Link-200.Britain for energy-dispersive X-ray spectroscopy (EDX).

In the process of the electrodes fabrication, one layer gas diffusion electrode was made. As-prepared manganese oxide was used as electrocatalyst. Na_2SO_4 (A.R) was used as pore-forming filler. A mixture containing the manganese oxide, graphite, acetylene black, Na_2SO_4, and PTFE (60% solution) with weight ratios of 4:1:1:4:1 was first mixed and grounded in excess ethanol. Then the mixture was placed onto a porous nickel substrate followed by roll-pressing it at 3×10^7 kg/cm^2 for 5 min to prepare cathode sheet. The thickness of the cathode sheet was controlled at 1∼4 mm. The sheet was then cut into a circular shape (2 cm in diameter) to prepare air cathode plate. A copper wire current collector (1 mm in diameter) was soldered to the center of the plate. As a comparison, electrolytic MnO_2 (battery grade EMD, I.C.No.2, Japan) was also used as electrocatalyst for preparation of air-electrode. A mixture containing the electrolytic MnO_2, graphite, acetylene black, Na_2SO_4 (A.R), and PTFE (60% solution) with same weight ratios was first mixed and grounded in excess ethanol. The electrode preparation was the same as the above-mentioned procedures.

Compacted zinc electrode was made of Zn powder (Toho Zinc Co. Ltd, Japan) and PTFE binder. The mixture, containing 2.5 g zinc powder and 60% PTFE solution, was placed onto a circular nickel substrate mesh (2 cm in diameter) followed by pressing it at 3×10^7 kg/cm^2 for 5 min to prepare anode plate. A current wire of copper was also soldered to the center of the plate.

Polarization curve, Chronnamperogram and Tafel plot tests of the air electrodes were carried out by CHI 660A electrochemical workstation system (CH Instrument, Cordova TN). Measurements were performed in a three-electrode cell with the air electrode as the working electrode, Hg/HgO electrode as the reference electrode and a platinum foil as the counter electrode. Polymer gel (potassium salt of cross-linked poly(acrylic acid) $[-CH_2CH(CO_2R)-]_n$, R = H or K, Aldrich) was used as electrolyte, which has been used in our previous experiment [18]. Electrochemical impedance spectroscopy and equivalent circuit investigation of air-electrode were performed by means of Autolab Modular Electrochemical Instruments (Autolab/PGSTAT30). The discharge characteristic of the zinc-air cell was characterized with galvanostatic charge-discharge unit (Arbins AT2042, USA). In the discharge measurements, test cells were fabricated according to our previous literature [18].

Results and discussion

X-ray diffraction (XRD) pattern of the as-prepared MnO_2 is shown in Fig. 1. The pattern indicated well-defined reflections, which means pure phase crystalline structure. The diffractive characteristic peaks of MnO_2 were assigned as 22.5° (120), 37.1° (131), 42.5° (300), 56.4° (160), and 67.2° (003). Structural analysis further revealed that the as-prepared MnO_2 was composed of typical hexagonal γ-MnO_2, which has the lattice parameters of $a = 6.36$ Å, $b = 10.15$ Å, $c = 4.09$ Å.

In order to investigate the composition of the MnO_2 nanosphere, EDX analysis was carried out. The results were shown in Fig. 2, which confirmed that the product

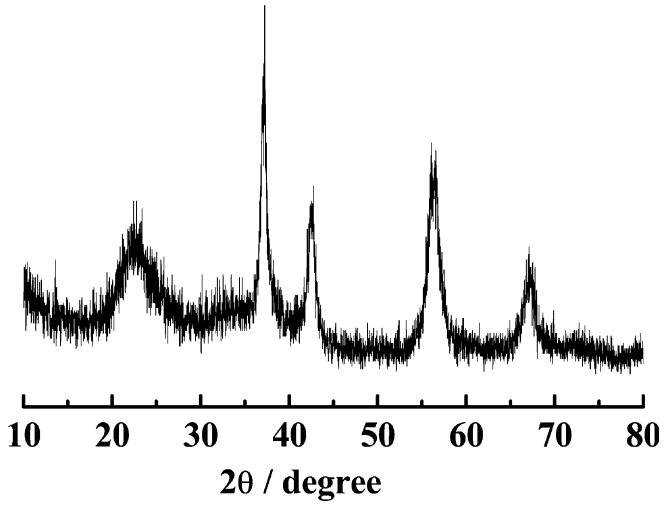

Fig. 1 X-ray diffraction (XRD) patterns of the prepared manganese oxide

contains only manganese and oxide elements. No other elements were detected.

It would be interesting to examine the morphology of the material, which has been in the form of powders. From SEM images in Fig. 3, at a low magnification, it can be seen that the material tends to form spherical particles having many flakes arranged uniformly to from the surface of each nanospheres, average nanosphere size of around ~1 μm. At a higher magnification of 100,000, SEM image of the as-prepared MnO_2 show the existence of the bird's nest morphologies and the nanostructured flakes. The nanosphere is actually made up of networks of solid flakes and pores with the size of 20~50 nm. Hollow [19] nanospheric manganese dioxide exhibits high surface area and has a number of nanopores. This morphology might be favorable for the oxygen reduction reaction. It is important to design a gas diffusion electrode that the electrolyte can penetrate into the pores without over-flooding them. Hollow nanospheric morphology like that of the as-prepared MnO_2 shown here would provide much convenience to the electrode design. The interconnected pores form channels for the electrolyte and air to move into the catalyst powders. This increases the three-phase, gas–liquid–solid, interfacial area and gives much more opportunity for oxygen dissolution and diffusion. Also, the presence of these hollow nanostructured particles results in materials having a high density of active sites for promoting fluid/solid reactions, and a hollow, open-weaved assembly, which provides a relatively easy path for percolation of the reactive fluid or gas through material. The short diffusion distance into and out of the chemically or catalytically active agglomerates ensures a high-reaction rate [20]. In addition, due to the nanograde radius of these channels, the capillary force would be strong enough to hold the electrolyte and prevent it from over flooding the electrode. Thus, the gas can reach the catalytic sites on the internal surfaces of the as-prepared MnO_2 while the electrolyte partially fills the channels. Therefore, this type of material would be an outstanding electrocatalytic material for oxygen reduction reaction.

The polarization characteristic of the air electrode with different manganese dioxide catalyst for the oxygen reduction is shown in Figs. 4 and 5. The cathode current for air electrode with EMD electrocatalyst starts to emerge at about 0 V and increase slowly as the potential become more negative, whereas the cathode current for the electrode employing as-prepared MnO_2 electrocatalyst starts to emerge at about the same voltage and increases rapidly as the potential become more negative. It is clear that the electrochemical processes are very similar for two catalysts used in our experiments. The difference in the profiles is only the difference of current produced during the electrochemical processes. The

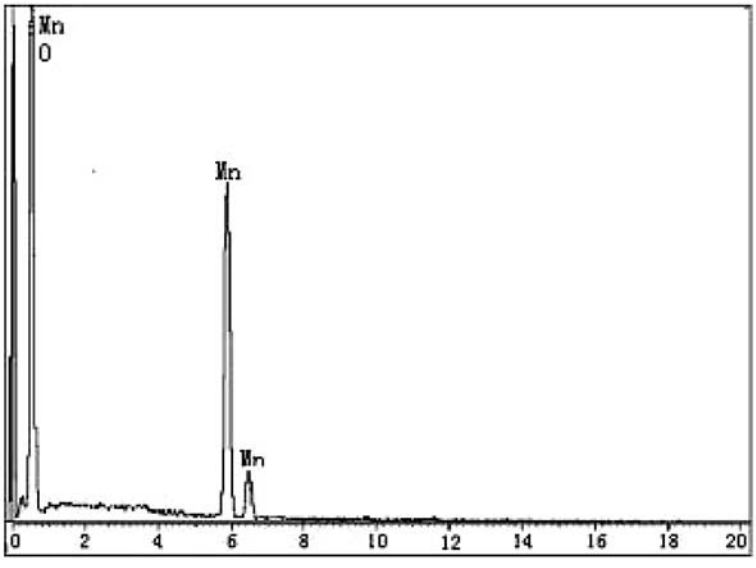

Fig. 2 Energy dispersion spectrometer (EDS) analysis of the prepared manganese oxide

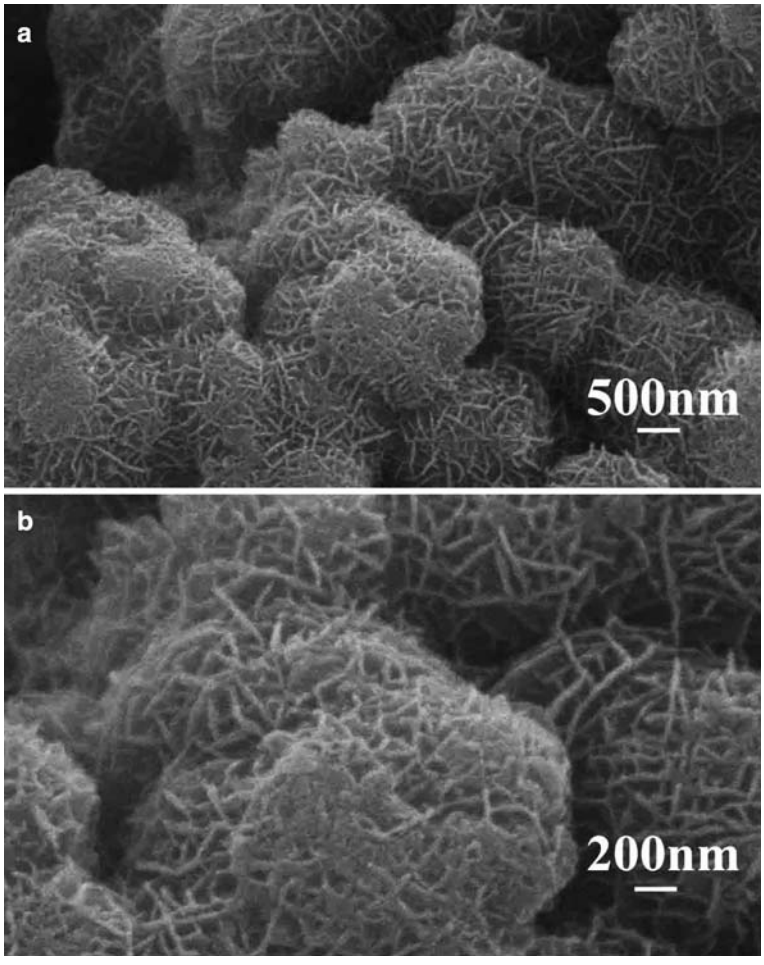

Fig. 3 Typical SEM images of the prepared manganese oxide
a 50,000× magnification
b 100,000×magnification

cathode current of latter is always higher than that of the former electrode (Fig. 4). Figure 5 shows the chronoamperometries for air electrodes using different catalysts. From Fig. 5, we can see that after applied −0.3 V potential, the cathode currents of the two air electrodes are all increased sharply within short time (0.1 s), and then achieve quickly to a stable value. However, the value of cathode current is quite different with respect to the different catalysts. The current value of the air electrode using as-prepared MnO_2 is significantly higher than that of air electrode employing EMD as the catalyst.

These results indicate that as-prepared MnO_2 has a better catalytic activity for oxygen reduction than that of EMD. The differences in polarization feature discussed above between the two electrodes may be attributed to the catalytic properties of the catalyst with different structures and morphologies. EMD used in the experiments

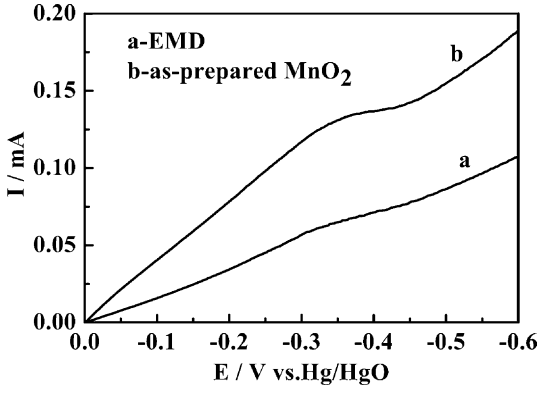

Fig. 4 Linear voltammograms of air electrodes using EMD and the prepared manganese oxide

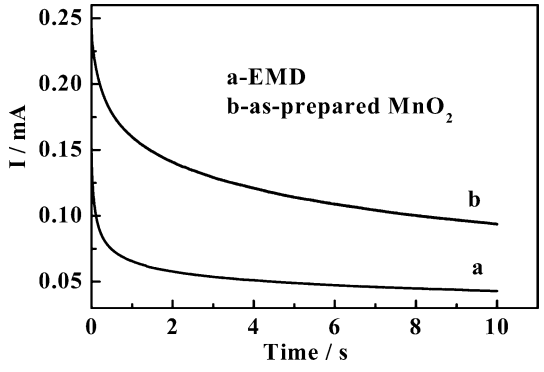

Fig. 5 Chronnamperogram for air electrodes using EMD and the prepared manganese oxide

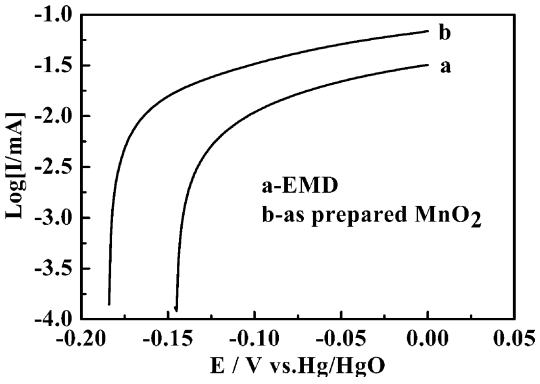

Fig. 6 Tafel plots of air electrodes using EMD and the prepared manganese oxide as catalyst

has normal particle size with irregular morphology [21]. The as-prepared MnO_2 was special hollow nanospherical particles and has the bird's nest morphologies of surface. This structure and morphology facilitate the oxygen to contact with catalyst and electrolyte sufficiently, subsequently, offers more active sites for oxygen reduction. This result is in agreement with the large current observed in the polarization curves of the oxygen electrode with the prepared MnO_2 as the catalyst.

As to the mechanism of oxygen reduction reaction (ORR) on MnO_2-catalysted air electrode, Yang et al. [22] has proposed that electrochemical reduction of oxygen can be expressed as follows:

$$MnO_2 + H_2O + e^- \Leftrightarrow MnOOH + OH^- \quad (1)$$

$$2MnOOH + O_2 \Leftrightarrow 2(MnOOH \cdot O^-) \quad (2)$$

$$(MnOOH \cdot O^-) + e^- \rightarrow MnO_2 + OH^- \quad (3)$$

So, the total reaction is: $O_2 + 2H_2O + 4e^- = 4OH^-$

Each mole of oxygen reduces to produce 4 mol of OH^- ions involving four-electron reduction process. Among these reactions, Eq. 3 is considered as rate-determining step and the reaction rate of oxygen reduction can be expressed in current density as:

$$i_c = 4FK_3K_2^{1/2}[O_2]^{1/2}m \times \frac{[OH^-]^{-1}\exp[-(1+\alpha)F/RT(E-E_0)]}{1+[OH^-]^{-}\exp[-F/RT(E-E_0)]} \quad (4)$$

Here, m is the total amount of Mn species at the surface of the catalyst. In our experiments, we examined Tafel behaviors of the EMD-catalysted and as-synthesized MnO_2-catalysted air electrodes. Tafel plots are shown in Fig. 6, from the Tafel data, we can see that the exchange current of as-synthesized MnO_2-catalysted air electrode is clearly higher than that of EMD-catalysted air electrode. In our experimental case, the electron transmission coefficient α can be considered equal, which can be calculated from the slops of the Tafel plots, the concentration of $[OH^-]$ and the other parameters for the two air electrodes can also be regarded as equal, thus, the difference of exchange currents between the two air electrodes is attributed to the difference of the value of $[O_2]^{1/2}m$, which reflects the opportunity for O_2 to contact with catalysts. In comparison with EMD, as-synthesized MnO_2 exhibits special spherical mesoporous morphology and has a hollow nanostructure, which can provide more spaces for O_2 to contact with catalyst, especially, high surface area of as-prepared MnO_2 (300 m^2/g) [19] contains much more Mn species. So, the value of $[O_2]^{1/2}m$ is more higher than that of EMD, consequently, the exchange current on as-prepared MnO_2-catalysted air electrode has a higher reflection. Generally, exchange current describes the kinetic parameters of electrode reaction; it can also express the absolute reaction rate of electrode reaction. The higher the exchange current, the easier the electrode reaction occurs. So, the oxygen reduction reaction on the as-prepared MnO_2-catalysted air electrode is easier than that on EMD-catalysted air electrode, i.e., as-prepared MnO_2 has a higher catalytic activity than EMD for ORR.

Typical AC impedance spectra for the air electrodes at an open-circuit voltage (OCV) are shown in Fig. 7. The Nyquist impedance spectra appear two different sizes of semicircles between the measuring frequencies. At a high frequency, besides the existence of induction, the Nyquist plot is composed of a small-depressed semicircle, which is attributed to the ohm polarization of the air electrode. At the low frequency, the semicircle is caused by the electrochemical polarization of the air electrode. It can also clearly be seen from the Nyquist plot that at low frequency, the plot has a tendency to change to a straight line that has an angle of 45°. This straight line is a characteristic of the semi-finite diffusion (Warburg impedance W). The electrolyte resistance is determined by the point of intersection of the high-frequency semicircle with the real axis.

The fitted circuit is shown (solid line) in Fig. 7, from the Fig. 7, we can see that the Fig. 8 represents the structure of the measured system and actually some kinetic parameters. According to above analysis, L_1 is inductance, R_1 is the electrolyte resistance between electrode surface and reference electrode, R_2 represents the surface contact resistance between electrode and electrolyte addition to ohm resistance of air electrode, here, Q_1 and Q_2, constant phase element caused by electrode roughness or by inhomogeneous reaction rates on electrode surface, represent respectively double-layer capacitance caused by ohmic polarization and Faraday reaction processes of the air electrode. R_3 describes electrochemical polarization resistance, W is diffusion impedance. The calculated kinetic parameters for air electrodes are given in Table 1. From this table, we can see clearly that the difference of electrolyte resistance (R_1) is very small for two air electrodes, whereas ohm resistance addition to interface resistance (R_2) and electrochemical polarization resistance (R_3) is clearly different. Especially, as-prepared MnO_2-catalysted air electrode has lower values of R_2 and R_3, higher value of W than that of the EMD-catalysted air electrode. These

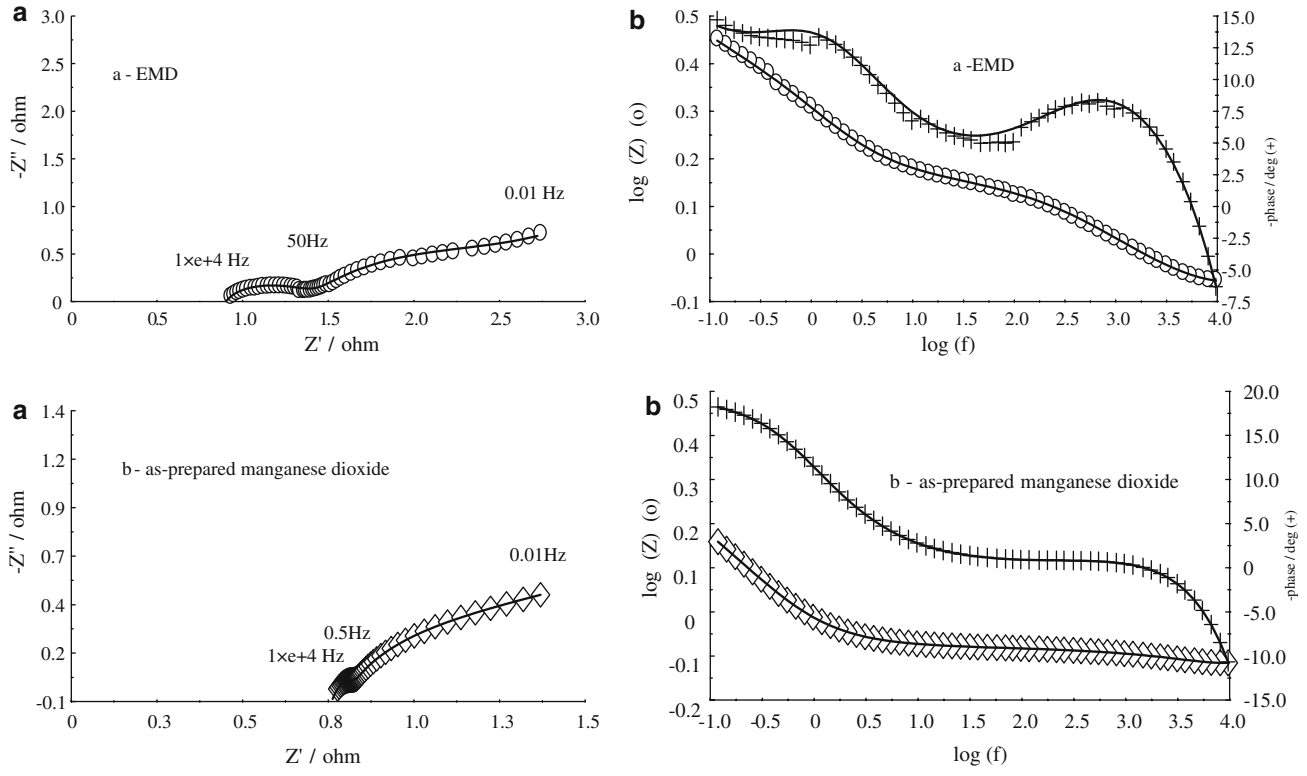

Fig. 7 The EIS spectra and Fitted EIS plots for air electrodes **a** Nequist Plot, **b** Bode Plot, a-EMD-catalysted air electrode, b-as-synthesized MnO_2-catalysted air electrode

results mean that the electrode process is controlled by kinetics for EMD-catalysted air electrode, whereas the electrode process is controlled mainly by diffusion for as-prepared MnO_2-catalysted air electrode; so, we can conclude that employing as-prepared MnO_2 as catalyst can decrease R_2 and R_3, i.e., as-prepared MnO_2 as catalyst is favorable to the oxygen reduction reaction, and this may be attributed to the high surface area, surface morphology, and hollow structure of the material. The AC impedance analysis result also further confirms that as-prepared MnO_2 has a higher catalytic activity for oxygen reduction reaction compared with the EMD. The result discussed here is also in agreement with that of polarization measurements for air electrodes.

As a kind of catalyst for zinc-air cell, it is very important to examine the behavior of catalyst in zinc-air cell system. Discharge profiles at the constant current of 157 mA (i.e., 50 mA/cm^2) are given in Fig. 9. During cell discharge, zinc at the anode is consumed by conversion to zinc oxide, and at the cathode, oxygen from the air is electrochemically reduced to hydroxide ions. The discharge capacity of the cell is limited by the amount of the anode zinc. So, the discharge performance of the cell is determined by the utilization rate of zinc.

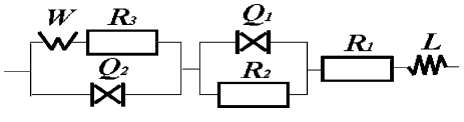

Fig. 8 Equivalent circuit of air electrode for the ac impedance analysis

From Fig. 9, we can see that the cells are able to sustain the current drains, as demonstrated by the flat discharge curves. At constant current drain of 62.4 mA (i.e., 20 mA/cm^2) and 157 mA (i.e., 50 mA/cm^2) for the cells, the open-circuit potential all reached about 1.2 V, the average working voltage plateaus were about 1.1 and 0.88 V for as-prepared MnO_2-catalysted cell, respectively. But for EMD-catalysted cell, the average working voltage plateaus were about 1.0 and 0.75 V. It is clear that the discharge voltage of the cell with as-prepared MnO_2 electrocatalyst is visibly higher than that of the cell with EMD electrocatalyst. The average working voltage of the former cell was promoted about 100$\sim$150 mV. Also as can be seen from these figures, the specific discharge capacity was also increased subsequently. Especially, specific discharge capacity of the former cell was clearly improved at high discharge rate, i.e., about equal to 222 mAh/g (as to mass of zinc) higher than that 91.7 mAh/g of the latter cell at 157 mA constant current. This result display that the former cell exhibited better utilization rate of zinc than the latter cell. From the changes of the specific discharge capacity with the discharge current for the Zinc-air cells with the different electrocatalysts, it was found that the former cell exhibited better discharge characteristics than the latter cell. These results indicate that the as-prepared MnO_2 electrocatalyst possess higher catalytic activity

Table 1 Electrode kinetic parameters modified by equivalent simulation

Air electrode	10^{-5} L_1 (H)	R_1 (Ω)	R_2 (Ω)	Q_1 Y_0, n	Q_2 Y_0, n	R_3 (Ω)	W (Ω)
EMD-catalysted	0.2688	0.791	0.583	0.5068e-3, $n=0.6233$	0.1367, $n=0.7546$	1.587	1.695
As-prepared MnO_2-catalysted	0.2730	0.719	0.2236	0.3434e-3, $n=0.5428$	0.8629, $n=0.7941$	0.325	2.204

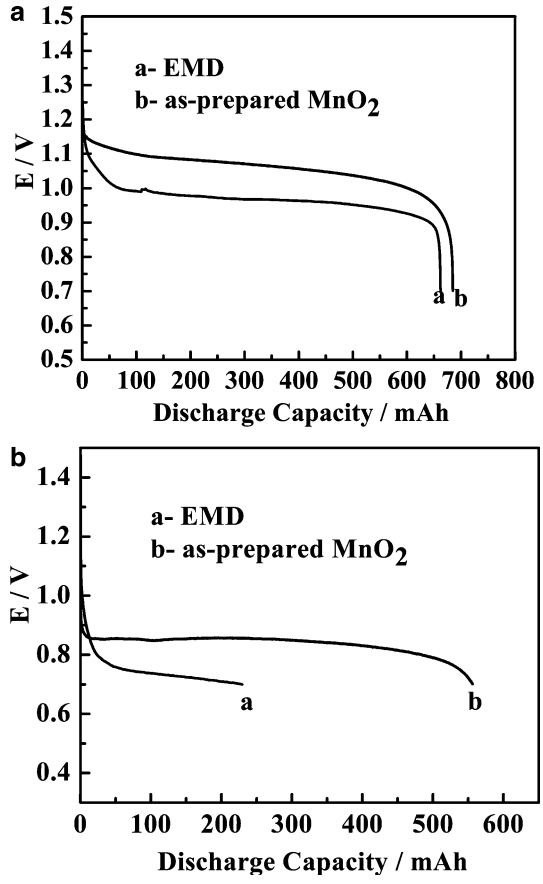

Fig. 9 The typical discharge curves of the Zinc-air cells using EMD and the prepared manganese oxide as catalyst **a** at 62.8 mA **b** at 157 mA constant discharge currents

than normal MnO_2. They are also in good agreement with that of polarization curve, Tafel plot, and electrochemical impedance spectra. The hollow, nanostructured features, along with the high surface area, might lead to superior properties for this transition-metal-oxide electrocatalyst.

Conclusions

In conclusion, mesoporous manganese dioxide with novel hollow nanospheric structure can be synthesized by a facile, template-free self-assembly process at room temperature in a short period of time. The as-prepared manganese dioxide has special mesoporous hollow nanospheric morphology and a typical composition of γ-MnO_2 as well as high surface area. These special properties contributed to its high electrocatalytic activity for oxygen reduction, which was characterized by polarization curve, Chronnamperogram, Tafel plot, and electrochemical impedance spectroscopy. An all solid-state zinc-air cell fabricated with this material as electrocatalyst for air electrode and potassium salt of cross-linked poly(acrylic acid) as an alkaline polymer gel electrolyte has a better discharge characteristic than that of cell employing EMD as the electrocatalyst. Along with the advantages of structure, morphology, and nanosized networks, using this material as electrocatalyst, might give rise to this type material of much desirable properties for potential application in zinc-air battery.

Acknowledgements Financial support from the "National Natural Science Foundation of China (No.60171004)" is gratefully acknowledged.

References

1. Zagal J, Bindra P, Yeager E (1980) J Electrochem Soc 127:1506
2. Appleby J, Savy M (1977) Electrochim Acta 22:1315
3. Iliev I, Gamburzev S, Kaisheva A (1986) J Power Sources 17:345
4. Shimizu Y, Uemura K, Matsuda H, Miura N, Yamazoe N(1990) J Electrochem Soc 137:3430
5. Hermann V, Dutriat D, Muller S, Comninellis Ch (2000) Electrochim Acta 46:365
6. Rao KV, Venkatesan VK, Udupa HVK (1982) J Electrochem Soc India 31–32:33
7. Gautier JL, Restovic A, Poillerat G, Chartier P (1997) Eur J Solid State Inorg Chem 34:367
8. Restovic A, Poillerat G, Chartier P, Gautier JL (1994) Electrochim Acta 39:1579
9. Zóltowski P, Drazic DM, Vorkapic L (1973) J Appl Electrochem 3:271
10. Kingsborough RP, Swager TM (2000) Chem Mater 12:872
11. Chang CJ, Deng Y, Shi C, Chang CK, Anson FC, Nocera DG(2000) Chem Commun 15:1355
12. Chung TD, Anson FC (2001) J Electroanal Chem 508:115
13. de Wolff PM (1959) Acta Crystallogr 12:341
14. Chabre Y, Pannetie J (1995) Prog Solid State Chem 23:1
15. Brock SL, Duan N, Tian ZR, Giraldo O, Zhou H, Suib SL (1998) Chem Mater 10:2619
16. Zhang Q (2001) Doctoral Dissertation, University of Connecticut, Storrs, CT
17. Bach S, Henry M, Baffier N, Livage J (1990) J Solid State Chem 88:325
18. Zhang GQ, Zhang XG (2004) Electrochim Acta 49:873
19. Yuan JK, Laubernds K, Zhang QH, Steven L (2003) J Am Chem Soc 125:4966
20. Xiao TD, Strutt PR, Kear BH, Chen HM, Wang DM (2003) US Patent 6,517, 802 B1
21. Kozawa A et al (1994) MnO_2 handbook. Sichuan Science and Technology Press, Chengdu, p 268
22. Cao YL, Yang HX, Ai XP, Xiao LF (2003) J Electroanal Chem 557:127